Mechanochemical Synthesis of Non-Solvated Dialkylalumanyl Anion and Solid-State-Characterization Using Crystallographic Analysis and X-ray Photoelectron Spectroscopy

Satoshi Kurumada,[a] Ryotaro Yamanashi,[a] Kengo Sugita,[a] Koji Kubota,[b,c] Hajime Ito,[b,c] Satoru Ikemoto,[d] Chaoqi Chen,[d] Takumi Moriyama,[d] Satoshi Muratugu,*[d,e] Mizuki Tada,[d,e,f] Takanori Koitaya,[g] Taisuke Ozaki,[h] Makoto Yamashita*[a,e]

[a] *Department of Molecular and Macromolecular Chemistry, Graduate School of Engineering, Nagoya University, Furo-cho, Chikusa-ku, Nagoya, 464-8603 Aichi, Japan*

[b] *Division of Applied Chemistry, Graduate School of Engineering, Hokkaido University, Sapporo, 060-8628 Hokkaido, Japan*

[c] *Institute for Chemical Reaction Design and Discovery (WPI-ICReDD), Hokkaido University, Sapporo, 060-8628 Hokkaido, Japan*

[d] *Department of Chemistry, Graduate School of Science & Research Center for Materials Science (RCMS), Nagoya University, Furo-cho, Chikusa-ku, Nagoya, 464-8603 Aichi, Japan*

[e] *Integrated Research Consortium on Chemical Science (IRCCS), Nagoya University, Furo-cho, Chikusa-ku, Nagoya, 464-8602 Aichi, Japan*

[f] *Research Center for Materials Science (RCMS), Nagoya University, Furo-cho, Chikusa-ku, Nagoya, 464-8602 Aichi, Japan*

[g] *Department of Chemistry, Graduate School of Science, Kyoto University, Kitashirakawa-Oiwake-cho, Sakyo-ku, Kyoto 606-8502, Japan*

[h] *The Institute for Solid State Physics, The University of Tokyo, 5-1-5 Kashiwanoha, Kashiwa, Chiba 277-8581, Japan*

ABSTRACT: A non-solvated alkyl-substituted Al(I) anion dimer was synthesized by a reduction of haloalumane precursor using a mechanochemical method. The crystallographic and theoretical analysis revealed its structure and electronic properties. Experimental and theoretical XPS analysis of the dimer with reference compounds revealed the low oxidation state of Al(I) anions. It should be emphasized that the experimentally obtained XPS binding energies were reproduced by delta SCF calculations and were linearly correlated with NPA charges and 2p orbital energies.

Aluminum (Al) is the most earth-abundant metal and is widely used in industry. Metallic aluminum in zero-oxidation state [Al(0)], obtained through electrolytic reduction of naturally produced stable Al(III) oxide, and alloy are valued as lightweight materials. In molecular chemistry, Al(III) compounds are often used as Lewis acid catalysts, hydride reagents, and alkyl nucleophiles.[1] In contrast to the rich chemistry of Al(III) molecules, the molecular chemistry of aluminum in a low oxidation state [Al(II) and Al(I)] has been developed in the last four decades.[2] All reported these molecules can be classified to three classes, radical anion,[3] base-stabilized neutral radical,[4,5] and dialumanes.[6] The history of the molecular Al(I) chemistry is relatively short because it has grown in the last 25 years.[7] There are three different types of Al(I) molecules (Chart 1): (a) a neutral Al compound with one σ-bond, one lone pair of electrons, and two vacant p-orbitals (referred to as alandiyl, alumylene, and aluminylene),[8] and its base-stabilized form and oligomers,[9] including **A** and $(Cp^*Al)_4$ as the most widely studied species; (b) dialumene, an Al=Al double bond species;[6s, 10] (c) alumanyl anion, an anionic Al(I) species having a lone pair of electrons on the Al atom.[11,12] After the first discovery of **B** in 2018,[11a] the chemistry of alumanyl anion has been rapidly developed in the past few years with a dianionic diamino or (alkyl)(amino) ligand,[11] including our latest contribution with a simple and scalable derivative **C**.[11k, 11l] In 2020, we also contributed to this chemistry with alkyl-substituted Al(I) anion **D** having a dianionic cyclic-alkylene ligand.[12]

Considering their low oxidation state, one can expect that these Al(II) and Al(I) species would exhibit distinct electronic properties on the Al atom in comparison with those of Al(III) species. To analyze the electronic structure of Al(I) species, Al K-edge XANES spectra of **A** and $(Cp^*Al)_4$ were measured to give its lower energy absorption than that of the corresponding Al(III) species.[13] Thus, analysis on the electronic property of Al(I) nuclei is limited to XANES analysis of neutral species.[14] The thermal instability of the previously reported **D** due to intramolecular C–H cleavage prevented its detailed characterization as Al(I) species. The latest development of mechanochemistry with an elemental metallic reductant for reductive C-C coupling,[15] preparation of Grignard

https://doi.org/10.26434/chemrxiv-2023-9h7z1 **ORCID:** https://orcid.org/0000-0002-3665-5311 Content not peer-reviewed by ChemRxiv. **License:** CC BY-NC-ND 4.0

reagent,[16] and formation of Mg(I) species[17] inspired us to apply the mechanochemical method to the synthesis of Al anions. Herein, we report the mechanochemical synthesis of non-solvated dialkylalumanyl anion **1** and a systematic study on the electronic structures of dialkyl- and diamino-Al(I), Al(II), and Al(III) species **1**-**6** (Chart 2) including newly synthesized dialumane **5** by using X-ray photoelectron spectroscopy (XPS) and DFT calculations.

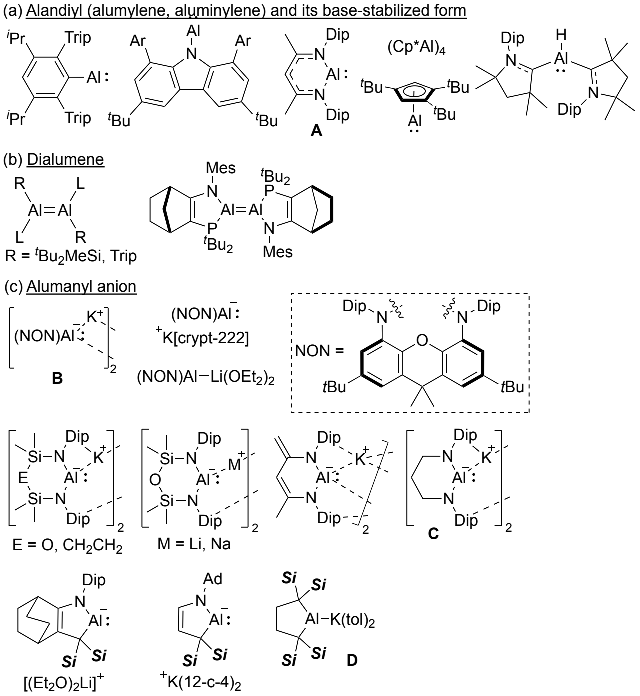

Chart 1. Molecular Al(I) species (Dip = 2,6-^{i}Pr$_2$C$_6$H$_3$, Trip = 2,4,6-^{i}Pr$_3$C$_6$H$_2$, Mes = 2,4,6-Me$_3$C$_6$H$_2$, Ad = 1-adamanthyl, ***Si*** = SiMe$_3$).

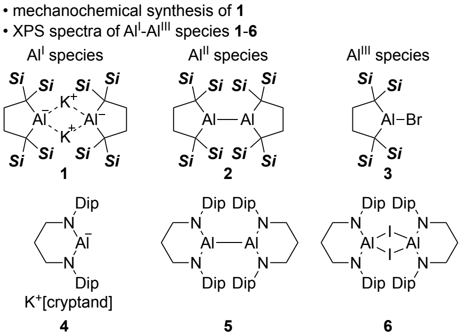

Chart 2. This work. (***Si*** = SiMe$_3$).

The dimeric alumanylpottassium **1** and symmetrical dialumane **5** were synthesized as illustrated in Scheme 1. The reaction of dilithiobutane **7** with AlBr$_3$ furnished dialkylaluminum bromide **3**. Ball-milling of **3** with Na/K alloy in the presence of a small amoun of hexamethyldisiloxane (TMS$_2$O) led to a formation of **1** as a red solid in 77% NMR yield. It should be noted that the reduction of **3** under conventional stirring condition in solution gave a trace amount of **1**. Recrystallization of **1** from the crude reaction mixture furnished red crystals of **1** in 20% isolated yield. The thermal stability of **1** up to ca. 80 °C is noteworthy, in contrast to the previously reported **D** decomposes in toluene solution at room temperature via C–H cleavage of toluene molecule.[12b] The single-crystal X-ray diffraction analysis of **1** revealed the centrosymmetric dimeric structure with two K--Al--K 3-center-2-electron bonds, supported by the shorter Al-K distance of 3.133(2) Å than a sum of covalent radii (4.36 Å for Al and K)[18] (Figure 1). This dimeric structural motif is similar to those of the previously reported diaminoalumanyl anions. The ^{1}H NMR spectrum of **1** and **3** indicates a C_s-symmetrical structure. Moreover, the ^{1}H NMR spectrum of **1** in toluene-d_8 gave an identical spectrum to that of the previously reported **D**, suggesting **1** was converted to the monomeric structure upon coordination of toluene. The signal at 230 ppm in ^{27}Al NMR spectrum of **3** in C$_6$D$_6$ was observed at a lower magnetic field than reported one of three coordinate Al(III) molecules, Mes$_3$Al (Mes = 2,4,6-trimethylphenyl),[19] whereases formally Al(I)-centered dialkylalumanyl anions **1** and **D** did not give any signals. The dialumane **5** was synthesized by a salt elimination reaction of previously reported **C**[11k] and **6**[11k] in 71% isolated yield. The Al–Al bond of 2.5988(5) Å in the crystal of **5** (See SI) was in the range of those [2.4946(9)[6k]-2.751(2)[6e] Å] of previously reported dialumanes.

Scheme 1. Synthesis of dimeric alumanylpotassium **1** and tetraaminodialumane **5** (***Si*** = SiMe$_3$, Dip = 2,6-^{i}Pr$_2$C$_6$H$_3$) ^{a}Yield in parentheses was determined by ^{1}H NMR with t-Bu$_3$C$_6$H$_3$ as an internal standard.

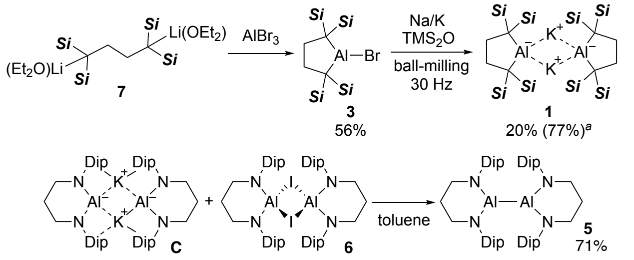

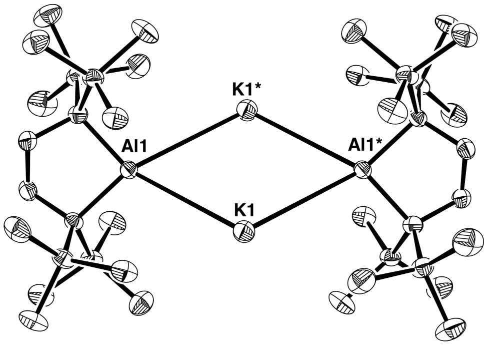

Figure 1. Molecular structure of **1** with thermal ellipsoids at 50% probability; all hydrogen atoms are omitted for clarity.

To reveal electronic structure of **1**-**6**, DFT calculations were performed at the B3LYP/def2svp level of theory (Figure 2). All molecules except for **4** were optimized for their one asymmetric unit obtained by crystallographic analysis, while **4** was optimized for its two asymmetric units to keep the interaction between the anionic aluminum atom and the K$^+$[cryptand] cation. The highest occupied molecular orbital (HOMO) of **1**

https://doi.org/10.26434/chemrxiv-2023-9h7z1 ORCID: https://orcid.org/0000-0002-3665-5311 Content not peer-reviewed by ChemRxiv. License: CC BY-NC-ND 4.0

is differently phased two lone pairs of electrons that are located mainly on the Al atom. The atoms in molecules analysis for **1** showed a polar character of the Al–K bond with a small ρ(r) value (0.010 e/a^3_0) and a positive $\nabla^2\rho(r)$ value (0.021 e/a^5_0). A natural population analysis (NPA) of **1** revealed that Al and K atoms are positively and differently charged (Al: +0.566, K: +0.838). Thus, the Al–K bond in **1** can be considered as a polarized bond between Al$^-$ and K$^+$. This characteristics are similar to those observed in the previously reported Al anions.[11,12] Similarly, the anionic parts of **4** possesses a lone-pair character at the Al centers with opposite phases for each Al atom. In contrast to that dialkyldialumane **2** has a significant contribution of the Al–Al bond to HOMO, diaminodialumane **5** exhibits non-bonding N–Al–N character. Bromoalumane **3** shows an antibonding combination between Al–C bond and a lone pair of electrons on the Br atom, while the dimeric iodoalumane **6** has non-bonding N–Al–N character.

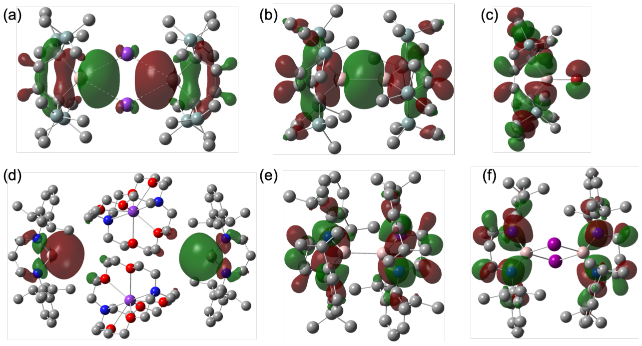

Figure 2. HOMOs of (a) **1**, (b) **2**, (c) **3**, (d) **4**,[a] (e) **5**, and (f) **6** calculated at B3LYP/def2svp level of theory.

[a] calculated for two asymmetric units.

It is suggested that the formal oxidation states of the Al atom in the Al anions **1** and **4** are I, those in dialumanes **2** and **5** are II, and those in haloalumanes **3** and **6** are III. To experimentally understand the difference in the Al oxidation states **1**-**6**, XPS spectra of **1**-**6** were measured (Figure 3). A single Al 2p XPS peak of Al(I) species, dialkyl-Al anion **1** and diamino-Al anion **4**, was observed at 74.0 eV (**1**) and 73.8 eV (**4**), respectively, which were much smaller than that of alumina [75.6 eV: Al(III)][20] and closer to that of aluminum foil [73.1 eV for Al 2p$_{1/2}$ and 72.7 eV for Al 2p$_{3/2}$: Al(0)],[21] supporting the reduced state of the Al(I) center in **1** and **4**. The Al 2p XPS peaks of **2** and **5** were observed at 75.4 eV (**2**) and 74.8 eV (**5**), respectively, which were larger than those of **1** and **4**, being consistent with that the Al(II) centers of **2** and **5** are electronically more positive than those of **1** and **4**. Similarly, the Al 2p XPS peaks of **3** and **6** exhibited the Al 2p XPS peak at 75.9 eV (**3**) and 75.2 eV (**6**), respectively, which are further increased, reflecting the most electronically positive characters of their Al centers among these Al species **1**-**6**. The core level of binding energies of **1**-**6** (for Al 2p and Br 3d states) were calculated by the delta SCF method[22] implemented in the OpenMX code.[23] The order of calculated binding energies (**1** < **2** < **3**, **4** < **5** < **6**) fit to that of experimentally obtained binding energies as summarized in Table 1. The means absolute error of the calculated binding energies vs. experimental data for **4**-**6** (0.11 eV) is smaller than that of **1**-**3** (0.53 eV). The delta SCF calculations could assign other peaks in **1** (KBr impurity, 69.44 eV) and **3** (Br bonded to Al, 70.81 eV) as well as peaks of Al foil [2p$_{3/2}$ 72.65 eV, 2p$_{1/2}$ 73.16 eV, surface Al$_2$O$_3$ 2p (av.) 76.07 eV]. Thus, it was experimentally and theoretically confirmed that the difference in Al oxidation states of **1**-**6** reflects binding energies in the XPS analysis, supporting the attribution of formal oxidation states of the Al centers in **1**-**6**.

The binding energies obtained by experimental XPS analysis were found to be correlated with NPA charges and energy levels of 2p orbitals (Table 1). As the XPS Al 2p binding energies increased, NPA charges increased as **1** < **2** < **3** and **4** < **5** < **6**. This is consistent with the increase of the formal oxidation states for these compounds. Furthermore, the energy levels of 2p-orbitals on the Al atom also increased in the same order. It should be emphasized that these values are linearly correlated with R^2 > 0.99 (Figure 4), although the accurate physical interpretation for this correlation should be studied in the future.

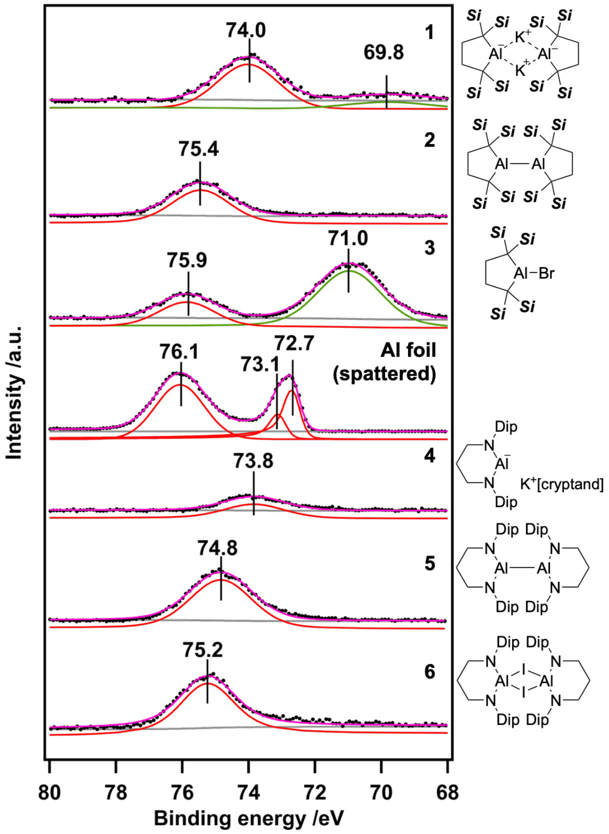

Figure 3. Al 2p XPS spectra of **1**-**6** and Al foil.[a] The peaks at 69.8 eV (for **1**) and 71.0 eV (for **3**) can be assigned to Br 3d core-levels of small impurities (KBr) of **1** and the bromide on the Al atom in **3**.

[a]Al foil was spattered to remove oxidized film from the surface (the peak at 76.1 eV can be assigned as the aluminum oxide on surface).

https://doi.org/10.26434/chemrxiv-2023-9h7z1 **ORCID:** https://orcid.org/0000-0002-3665-5311 Content not peer-reviewed by ChemRxiv. **License:** CC BY-NC-ND 4.0

Table 1. Summary of experimentally obtained binding energy by XPS measurement, calculated binding energy using delta SCF method, calculated NPA charges and energy of 2p orbital on Al atom at the B3LYP/def2svp level of theory.

compound	1	2	3	4	5	6
Binding energy in XPS analysis (eV)	74.0	75.4	76.1	73.8[a]	74.8	75.2
Calculated binding energy (eV)[b]	74.14	74.53	75.53	73.97	74.68	75.24
NPA charges on Al	0.566	1.254	1.692	0.552[a]	1.278	1.550
Calculated energy (eV) of 2p orbital on Al[c]	−74.9	−76.6	−77.9	−73.1[a]	−76.0	−76.8

[a] calculated for two asymmetric units, [b] avaraged values from those of $2p_{3/2}$ and $2p_{1/2}$ states with consideration of degeneracy, [c] calculated as an avarage of core $2p_x$, $2p_y$, and $2p_z$ orbitals from NBO analysis.

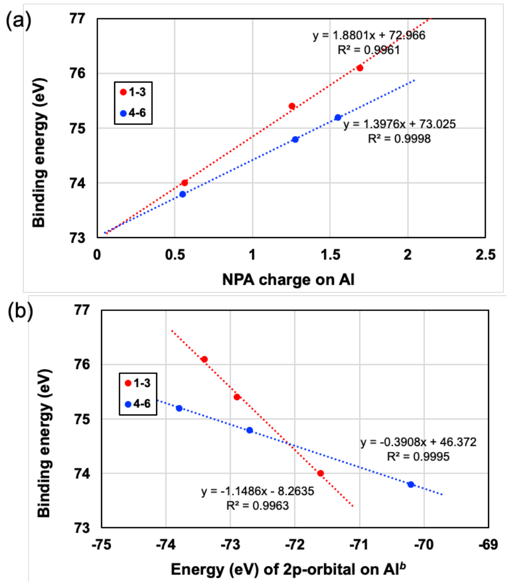

Figure 4. Linear relationship between the observed binding energy in XPS analysis and (a) NPA charge on the Al atom, or (b) the energy levels of the calculated 2p-orbitals of Al atom.

In conclusion, we reported the synthesis of dialkylalumanylpotassium dimer **1** with ball-milling reduction. A combination of the X-ray structural analysis and DFT calculations revealed the electronic structure of **1** with a contribution of lone-pair and vacant 3p-orbital on the Al(I) center. Experimental and theoretical XPS analysis of Al anions, dialumanes, and haloalumanes revealed their different Al 2p binding energies, depending on the difference in the oxidation states. The experimentally observed XPS binding energies were also found to be linearly correlated with calculated NPA charges and 2p energy levels of the Al atom, which fairly supported the attribution of Al formal oxidation states. These findings would open new ways to investigate unusual oxidation states of main group element chemistry and a reference dataset for Al(I) and Al(II) species for XPS analysis.

ASSOCIATED CONTENT

Supporting Information

The Supporting Information is available free of charge on the ACS Publications website.

Experimental and computational details (PDF)

Crystallographic data for **1**, **3**, and **5** (CIF)

DFT coordinates (XYZ)

AUTHOR INFORMATION

Corresponding Author

* smuratsugu@chem.nagoya-u.ac.jp, muratsugu.satoshi.a5@f.mail.nagoya-u.ac.jp
* makoto@oec.chembio.nagoya-u.ac.jp

Notes

The authors declare no competing financial interest.

ACKNOWLEDGMENT

This research was supported by a Grant-in-Aid for Scientific Research (B) (21H01915 for M.Y.), Grant-in-Aid for Exploratory Research (22H00335 for S.M.), Grant-in-Aid for Scientific Research on Innovative Areas (20H04808 [hybrid catalysis] for S.M.), Grant-in-Aid for Scientific Research (B) (23H01937 for S.M.), JST CREST grant (JPMJCR19R1 for H.I.), and JST FOREST grant (JPMJFR201I for K.K.). S.K. and R.Y. are grateful for a JSPS research fellowship (202115731, 22J23885). The computation was performed using Research Centre for Computational Science, Okazaki, Japan (Project: 21-IMS-C222, 22-IMS-C006). The XPS measurement was conducted at the Institute for Molecular Science, supported by the Nanotechnology Platform Program <Molecule and Material Synthesis> (JPMXP09S21MS1061) and <Advanced Research Infrastructure for Materials Nanotechnology> (JPMXP1222MS1011 and JPMXP1223MS1023) of MEXT, Japan.

REFERENCES AND NOTES

1. Saito, S., Aluminum in Organic Synthesis. In *Main Group Metals in Organic Synthesis*, 2004; pp 189-306.

2. Inorganic AlX compounds (X = halogen) have been studied as "aluminum subhalides" although their "molecular" structures have not been reported. a) Tacke, M.; Schnoeckel, H. Metastable aluminum chloride, AlCl, as a solid and in solution. Inorg. Chem. 1989, 28, 2895-2896. b) Schnockel, H. IR Absoption of AlCl and AlBr in solid noble-gases. Z. Naturforsch., B: Chem. Sci. 1976, 31, 1291-1292. c) Wyse, F. C.; Gordy, W. Millimeter Wave Rotational Spectra of AlCl, AlBr, and AlI. J. Chem. Phys. 1972, 56, 2130-2136.

3. Nakamoto, M.; Yamasaki, T.; Sekiguchi, A. Stable Mononuclear Radical Anions of Heavier Group 13 Elements: $[(^t\mathrm{Bu}_2\mathrm{MeSi})_3\mathrm{E}^{\cdot-}]\cdot[\mathrm{K}^+(2.2.2\text{-Cryptand})]$ (E = Al, Ga). *J. Am. Chem. Soc.* **2005**, *127*, 6954-6955.

4. Henke, P.; Pankewitz, T.; Klopper, W.; Breher, F.; Schnöckel, H. Snapshots of the Al-Al σ-Bond Formation Starting from $\{AlR_2\}$ Units: Experimental and Computational Observations. *Angew. Chem. Int. Ed.* **2009**, *48*, 8141-8145.

5. Related CAAC-stabilized aluminum radicals were reported to have negligible spin density on the Al center with Al(III) character due to delocalization of spin to the CAAC moiety [CAAC = cyclic (alkyl)(amino)carbene]. a) Kundu, S.; Sinhababu, S.; Dutta, S.; Mondal, T.; Koley, D.; Dittrich, B.; Schwederski, B.; Kaim, W.; Stückl, A. C.; Roesky, H. W. Synthesis and characterization of Lewis base stabilized mono- and diorgano aluminum radicals. *Chem. Commun.* **2017**, *53*, 10516-10519. b) Li, B.; Kundu, S.; Stückl, A. C.; Zhu, H.; Keil, H.; Herbst-Irmer, R.; Stalke, D.; Schwederski, B.; Kaim, W.; Andrada, D. M.; Frenking, G.; Roesky, H. W. A

https://doi.org/10.26434/chemrxiv-2023-9h7z1 **ORCID:** https://orcid.org/0000-0002-3665-5311 Content not peer-reviewed by ChemRxiv. **License:** CC BY-NC-ND 4.0

Stable Neutral Radical in the Coordination Sphere of Aluminum. *Angew. Chem. Int. Ed.* **2017**, *56*, 397-400.

6. (a) Uhl, W. Tetrakis[bis(trimethylsilyl)methyl]dialane(4), a Compound with an Aluminium-Aluminium Bond. *Z. Naturforsch., B: Chem. Sci.* **1988,** *43*, 1113-1118; (b) Wehmschulte, R. J.; Ruhlandt-Senge, K.; Olmstead, M. M.; Hope, H.; Sturgeon, B. E.; Power, P. P. Reduction of a tetraaryldialane to generate aluminum-aluminum π-bonding. *Inorg. Chem.* **1993,** *32*, 2983-2984; (c) Mocker, M.; Robl, C.; Schnöckel, H. Donor-Stabilized Aluminum(II) Bromide. *Angew. Chem. Int. Ed. Engl.* **1994,** *33*, 862-863; (d) Ecker, A.; Baum, E.; Friesen, M. A.; Junker, M. A.; Üffing, C.; Köppe, R.; Schnöckel, H. Synthesen und Strukturen donorstabilisierter Aluminiumdihalogenide. *Z. Anorg. Allg. Chem.* **1998,** *624*, 513-516; (e) Wiberg, N.; Amelunxen, K.; Blank, T.; Nöth, H.; Knizek, J. Tetrasupersilyldialuminum $[(t\text{-Bu})_3Si]_2Al\text{-}Al[Si(t\text{-Bu})_3]_2$: The Dialane(4) with the Longest Al-Al Bond to Date. *Organometallics* **1998,** *17*, 5431-5433; (f) Klemp, C.; Stößer, G.; Krossing, I.; Schnöckel, H. $Al_5Br_7{\cdot}5$ THF-The First Saltlike Aluminum Subhalide. *Angew. Chem. Int. Ed.* **2000,** *39*, 3691-3694; (g) Klemp, C.; Üffing, C.; Baum, E.; Schnöckel, H. Synthese und Struktur gemischt-substituierter Dialane $Al_2X_2\{Si(SiMe_3)_3\}_2{\cdot}2\,THF$ (X=Cl, Br). *Z. Anorg. Allg. Chem.* **2000,** *626*, 1787-1791; (h) Klimek, K. S.; Cui, C.; Roesky, H. W.; Noltemeyer, M.; Schmidt, H.-G. Synthesis and Characterization of 1-Aza-allyl Complexes with Al−Al, Ga−Ga, and In−In Bonds. *Organometallics* **2000,** *19*, 3085-3090; (i) Wright, R. J.; Phillips, A. D.; Power, P. P. The [2+4] Diels-Alder Cycloadditon Product of a Probable Dialuminene, Ar‘AlAlAr‘ (Ar‘ = C_6H_3-2,6-$Dipp_2$; Dipp = C_6H_3-2,6-Pr^i_2), with Toluene. *J. Am. Chem. Soc.* **2003,** *125*, 10784-10785; (j) Vollet, J.; Burgert, R.; Schnöckel, H. $Al_{20}Cp^*_8X_{10}$ (X=Cl, Br): Snapshots of the Formation of Metalloid Clusters from Polyhedral Al_nX_m Molecules? *Angew. Chem. Int. Ed.* **2005,** *44*, 6956-6960; (k) Cui, C.; Li, X.; Wang, C.; Zhang, J.; Cheng, J.; Zhu, X. Isolation of a 1,2-Dialuminacyclobutene. *Angew. Chem. Int. Ed.* **2006,** *45*, 2245-2247; (l) Minasian, S. G.; Arnold, J. Synthesis and reactivity of bis-pentamethylcyclopentadienyl diiododialane $(Cp^*AlI)_2$: an aluminium(ii) precursor to $(Cp^*Al)_4$. *Chem. Commun.* **2008**, 4043-4045; (m) Bonyhady, S. J.; Collis, D.; Frenking, G.; Holzmann, N.; Jones, C.; Stasch, A. Synthesis of a stable adduct of dialane(4) (Al_2H_4) via hydrogenation of a magnesium(I) dimer. *Nat. Chem.* **2010,** *2*, 865-869; (n) Fedushkin, I. L.; Moskalev, M. V.; Lukoyanov, A. N.; Tishkina, A. N.; Baranov, E. V.; Abakumov, G. A. Dialane with a Redox-Active Bis-amido Ligand: Unique Reactivity towards Alkynes. *Chem. Eur. J.* **2012,** *18*, 11264-11276; (o) Zhao, Y.; Liu, Y.; Yang, L.; Yu, J. G.; Li, S.; Wu, B.; Yang, X. J. Mechanistic Insight into the N-N Bond‐Cleavage of Azo-Compounds that was Induced by an Al-Al-bonded Compound $[L^{2-}Al^{II}\text{-}Al^{II}L^{2-}]$. *Chem. Eur. J.* **2012,** *18*, 6022-6030; (p) Agou, T.; Nagata, K.; Tokitoh, N. Synthesis of a Dialumene-Benzene Adduct and Its Reactivity as a Synthetic Equivalent of a Dialumene. *Angew. Chem. Int. Ed.* **2013,** *52*, 10818-10821; (q) Haider, W.; Andrada, D. M.; Bischoff, I.-A.; Huch, V.; Schäfer, A. A bis(aluminocenophane) with a short aluminum–aluminum single bond. *Dalton Trans.* **2019,** *48*, 14953-14957; (r) Kretsch, J.; Kreyenschmidt, A.; Schillmöller, T.; Herbst-Irmer, R.; Stalke, D. Mixed Low-Valent Alanes from the Bis(4-methyl-benzoxazol-2-yl)methanide Ligand. *Inorg. Chem.* **2020,** *59*, 13690-13699; (s) Weetman, C.; Porzelt, A.; Bag, P.; Hanusch, F.; Inoue, S. Dialumenes – aryl vs. silyl stabilisation for small molecule activation and catalysis. *Chem. Sci.* **2020,** *11*, 4817-4827; (t) Li, B.; Geoghegan, B. L.; Weinert, H. M.; Wölper, C.; Cutsail, G. E.; Schulz, S. Synthesis and redox activity of carbene-coordinated group 13 metal radicals. *Chem. Commun.* **2022,** *58*, 4372-4375.

7. Jones, C.; Stasch, A., The Chemistry of the Group 13 Metals in the +1 Oxidation State. In *The Group 13 Metals Aluminium, Gallium, Indium and Thallium: Chemical Patterns and Peculiarities*, Aldridge, S.; Downs, A. J., Eds. Wiley: 2011; pp 285-341.

8. (a) Queen, J. D.; Lehmann, A.; Fettinger, J. C.; Tuononen, H. M.; Power, P. P. The Monomeric Alanediyl :$AlAr^iPr_8$ (Ar^iPr_8 = C_6H-2,6-(C_6H_2-2,4,6-Pr^i_3)$_2$-3,5-Pr^i_2): An Organoaluminum(I) Compound with a One-Coordinate Aluminum Atom. *J. Am. Chem. Soc.* **2020,** *142*, 20554-20559; (b) Zhang, X.; Liu, L. L. Modulating the Frontier Orbitals of an Aluminylene for Facile Dearomatization of Inert Arenes. *Angew. Chem. Int. Ed.* **2022,** *61*, e202116658.

9. (a) Dohmeier, C.; Robl, C.; Tacke, M.; Schnöckel, H. The Tetrameric Aluminum(I) Compound [{Al(η 5 ‐ C5Me5)}4]. *Angew. Chem. Int. Ed. Engl.* **1991,** *30*, 564-565; (b) Dohmeier, C.; Loos, D.; Schnöckel, H. Aluminum(I) and Gallium(I) Compounds: Syntheses, Structures, and Reactions. *Angew. Chem. Int. Ed. Engl.* **1996,** *35*, 129-149; (c) Cui, C.; Roesky, H. W.; Schmidt, H. G.; Noltemeyer, M.; Hao, H.; Cimpoesu, F. Synthesis and Structure of a Monomeric Aluminum(I) Compound $[\{HC(CMeNAr)_2\}Al]$ (Ar=2,6–$^iPr_2C_6H_3$): A Stable Aluminum Analogue of a Carbene. *Angew. Chem. Int. Ed.* **2000,** *39*, 4274-4276; (d) Hofmann, A.; Tröster, T.; Kupfer, T.; Braunschweig, H. Monomeric $Cp^{3t}Al$(I): synthesis, reactivity, and the concept of valence isomerism. *Chem. Sci.* **2019,** *10*, 3421-3428; (e) Mellerup, S. K.; Cui, Y.; Fantuzzi, F.; Schmid, P.; Goettel, J. T.; Bélanger-Chabot, G.; Arrowsmith, M.; Krummenacher, I.; Ye, Q.; Engel, V.; Engels, B.; Braunschweig, H. Lewis-Base Stabilization of the Parent Al(I) Hydride under Ambient Conditions. *J. Am. Chem. Soc.* **2019,** *141*, 16954-16960.

10. (a) Bag, P.; Porzelt, A.; Altmann, P. J.; Inoue, S. A Stable Neutral Compound with an Aluminum–Aluminum Double Bond. *J. Am. Chem. Soc.* **2017,** *139*, 14384-14387; (b) Falconer, R. L.; Byrne, K. M.; Nichol, G. S.; Krämer, T.; Cowley, M. J. Reversible Dissociation of a Dialumene. *Angew. Chem. Int. Ed.* **2021,** *60*, 24702-24708.

11. (a) Hicks, J.; Vasko, P.; Goicoechea, J. M.; Aldridge, S. Synthesis, structure and reaction chemistry of a nucleophilic aluminyl anion. *Nature* **2018,** *557*, 92-95; (b) Hicks, J.; Vasko, P.; Goicoechea, J. M.; Aldridge, S. Reversible, Room-Temperature C-C Bond Activation of Benzene by an Isolable Metal Complex. *J. Am. Chem. Soc.* **2019,** *141*, 11000-11003; (c) Schwamm, R. J.; Anker, M. D.; Lein, M.; Coles, M. P. Reduction vs. Addition: The Reaction of an Aluminyl Anion with 1,3,5,7‐Cyclooctatetraene. *Angew. Chem. Int. Ed.* **2019,** *58*, 1489-1493; (d) Schwamm, R. J.; Coles, M. P.; Hill, M. S.; Mahon, M. F.; McMullin, C. L.; Rajabi, N. A.; Wilson, A. S. S. A Stable Calcium Alumanyl. *Angew. Chem. Int. Ed.* **2020,** *59*, 3928-3932; (e) Koshino, K.; Kinjo, R. Construction of σ-Aromatic AlB_2 Ring via Borane Coupling with a Dicoordinate Cyclic (Alkyl)(Amino)Aluminyl Anion. *J. Am. Chem. Soc.* **2020,** *142*, 9057-9062; (f) Grams, S.; Eyselein, J.; Langer, J.; Färber, C.; Harder, S. Boosting Low-Valent Aluminum(I) Reactivity with a Potassium Reagent. *Angew. Chem. Int. Ed.* **2020,** *59*, 15982-15986; (g) Roy, M. M. D.; Hicks, J.; Vasko, P.; Heilmann, A.; Baston, A.-M.; Goicoechea, J. M.; Aldridge, S. Probing the Extremes of Covalency in M−Al bonds: Lithium and Zinc Aluminyl Compounds. *Angew. Chem. Int. Ed.* **2021,** *60*, 22301-22306; (h) Evans, M. J.; Anker, M. D.; McMullin, C. L.; Neale, S. E.; Coles, M. P. Dihydrogen Activation by Lithium- and Sodium-Aluminyls. *Angew. Chem. Int. Ed.* **2021,** *60*, 22289-22292; (i) Gentner, T. X.; Evans, M. J.; Kennedy, A. R.; Neale, S. E.; McMullin, C. L.; Coles, M. P.; Mulvey, R. E. Rubidium and caesium aluminyls: synthesis, structures and reactivity in C–H bond activation of benzene. *Chem. Commun.* **2022,** *58*, 1390-1393; (j) Yan, C.; Kinjo, R. A Three-Membered Diazo-Aluminum Heterocycle to Access an Al=C π Bonding Species. *Angew. Chem. Int. Ed.* **2022,** *61*, e202211800; (k) Feng, G.; Chan, K. L.; Lin, Z.; Yamashita, M. Al–Sc Bonded Complexes: Synthesis, Structure, and Reaction with Benzene in the Presence of Alkyl Halide. *J. Am. Chem. Soc.* **2022,** *144*, 22662-22668; (l) Feng, G.; Yamashita, M. Alkali Chloride Adducts of Acyclic Acylaluminum: Synthesis, Structure, and Reactivity Studies. *Angew. Chem. Int. Ed.* **2023,** *62*, e202306366.

12. (a) Kurumada, S.; Takamori, S.; Yamashita, M. An alkyl-substituted aluminium anion with strong basicity and nucleophilicity. *Nat. Chem.* **2020,** *12*, 36-39; (b) Kurumada, S.; Sugita, K.; Nakano, R.; Yamashita, M. A meta-Selective C−H Alumination of Mono-Substituted Benzene by Using An Alkyl-Substituted Al Anion through Hydride-Eliminating S_NAr Reaction. *Angew. Chem. Int. Ed.* **2020,** *59*, 20381-20384; (c) Sugita, K.; Nakano, R.; Yamashita, M. Cycloaddition of Dialkylalumanyl Anion toward Unsaturated Hydrocarbons in (1+2) and (1+4) Modes. *Chem. Eur. J.* **2020,** *26*, 2174-2177; (d) Sugita, K.; Yamashita, M. An Alumanylyttrium Complex with an Absorption due to a Transition from the Al−Y Bond to an Unoccupied d-Orbital. *Chem. Eur. J.* **2020,** *26*, 4520-4523; (e) Sugita, K.; Yamashita, M. One-Electron Reduction of Ti(IV) Complex by Dialkylaluminum(I) Anion Giving the Ti(III) Species. *Organometallics* **2020,** *39*, 2125-2129; (f) Kurumada, S.; Yamashita, M. A Tetraorganyl-

https://doi.org/10.26434/chemrxiv-2023-9h7z1 **ORCID:** https://orcid.org/0000-0002-3665-5311 Content not peer-reviewed by ChemRxiv. **License:** CC BY-NC-ND 4.0

Alumaborane with An Al–B σ-Bond and Two Adjacent Lewis-Acidic Centers. *J. Am. Chem. Soc.* **2022,** *144*, 4327-4332.

13. (a) Altman, A. B.; Pemmaraju, C. D.; Camp, C.; Arnold, J.; Minasian, S. G.; Prendergast, D.; Shuh, D. K.; Tyliszczak, T. Theory and X-ray Absorption Spectroscopy for Aluminum Coordination Complexes - Al K-Edge Studies of Charge and Bonding in (BDI)Al, (BDI)AlR_2, and (BDI)AlX_2 Complexes. *J. Am. Chem. Soc.* **2015,** *137*, 10304-10316; (b) Minasian, S. G.; Krinsky, J. L.; Rinehart, J. D.; Copping, R.; Tyliszczak, T.; Janousch, M.; Shuh, D. K.; Arnold, J. A Comparison of 4f vs 5f Metal−Metal Bonds in $(CpSiMe_3)_3M$−ECp* (M = Nd, U; E = Al, Ga; Cp* = C_5Me_5): Synthesis, Thermodynamics, Magnetism, and Electronic Structure. *J. Am. Chem. Soc.* **2009,** *131*, 13767-13783.

14. A related XANES analysis of nontrigonal P(III) molecules was reported. See: Lee, K.; Blake, A. V.; Tanushi, A.; McCarthy, S. M.; Kim, D.; Loria, S. M.; Donahue, C. M.; Spielvogel, K. D.; Keith, J. M.; Daly, S. R.; Radosevich, A. T. Validating the Biphilic Hypothesis of Nontrigonal Phosphorus(III) Compounds. *Angew. Chem. Int. Ed.* **2019**, *58*, 6993-6998.

15. Nicholson, W. I.; Howard, J. L.; Magri, G.; Seastram, A. C.; Khan, A.; Bolt, R. R. A.; Morrill, L. C.; Richards, E.; Browne, D. L. Ball-Milling-Enabled Reactivity of Manganese Metal. *Angew. Chem. Int. Ed.* **2021,** *60*, 23128-23133.

16. (a) Takahashi, R.; Hu, A.; Gao, P.; Gao, Y.; Pang, Y.; Seo, T.; Jiang, J.; Maeda, S.; Takaya, H.; Kubota, K.; Ito, H. Mechanochemical synthesis of magnesium-based carbon nucleophiles in air and their use in organic synthesis. *Nat. Commun.* **2021,** *12*, 6691; (b) Harrowfield, J. M.; Hart, R. J.; Whitaker, C. R. Magnesium and Aromatics: Mechanically-Induced Grignard and McMurry Reactions. *Aust. J. Chem.* **2001,** *54*, 423-425; (c) Birke, V.; Schutt, C.; Burmeier, H.; Ruck, W. K. L. Defined Mechanochemical Reductive Dechlorination of 1,3,5-Trichlorobenzene at Rroom Temperature in A Ball Mill. *Fresenius Environ. Bull.* **2011,** *20*, 2794-2805; (d) Speight, I. R.; Hanusa, T. P. Exploration of Mechanochemical Activation in Solid-State Fluoro-Grignard Reactions. *Molecules* **2020,** *25*, 570; (e) Pfennig, V. S.; Villella, R. C.; Nikodemus, J.; Bolm, C. Mechanochemical Grignard Reactions with Gaseous CO2 and Sodium Methyl Carbonate. *Angew. Chem. Int. Ed.* **2022,** *61*, e202116514; (f) Varma Nallaparaju, J.; Nikonovich, T.; Jarg, T.; Merzhyievskyi, D.; Aav, R.; Kananovich, D. G. Mechanochemistry-Amended Barbier Reaction as an Expedient Alternative to Grignard Synthesis. *Angew. Chem. Int. Ed.* **2023,** *61*, e202305775.

17. (a) Jędrzkiewicz, D.; Mai, J.; Langer, J.; Mathe, Z.; Patel, N.; DeBeer, S.; Harder, S. Access to a Labile Monomeric Magnesium Radical by Ball-Milling. *Angew. Chem. Int. Ed.* **2022,** *61*, e202200511; (b) Jędrzkiewicz, D.; Langer, J.; Harder, S. Low-valent Mg(I) complexes by ball-milling. *Z. Anorg. Allg. Chem.* **2022,** *648*, e202200138.

18. Emsley, J., *The Elements*. 3rd ed.; Oxford University Press: New York, 1998.

19. Jerius, J. J.; Hahn, J. M.; Rahman, A. F. M. M.; Mols, O.; Ilsley, W. H.; Oliver, J. P. Synthesis, molecular structure, and NMR spectra of trimesitylaluminum, a novel molecule with three coordinate aluminum. *Organometallics* **1986,** *5*, 1812-1814.

20. Olefjord, I.; Mathieu, H. J.; Marcus, P. Intercomparison of surface analysis of thin aluminium oxide films. *Surf. Interface Anal.* **1990,** *15*, 681-692.

21. Rotole, J. A.; Sherwood, P. M. A. Aluminum Foil by XPS. *Surf. Sci. Spectra* **1998,** *5*, 4-10.

22. Ozaki, T.; Lee, C.-C. Absolute Binding Energies of Core Levels in Solids from First Principles. *Phys. Rev. Lett.* **2017,** *118*, 026401.

23. Ozaki, T. Variationally optimized atomic orbitals for large-scale electronic structures. *Phys. Rev. B* **2003,** *67*, 155108.

https://doi.org/10.26434/chemrxiv-2023-9h7z1 **ORCID:** https://orcid.org/0000-0002-3665-5311 Content not peer-reviewed by ChemRxiv. **License:** CC BY-NC-ND 4.0

Authors are required to submit a graphic entry for the Table of Contents (TOC) that, in conjunction with the manuscript title, should give the reader a representative idea of one of the following: A key structure, reaction, equation, concept, or theorem, etc., that is discussed in the manuscript. Consult the journal's Instructions for Authors for TOC graphic specifications.

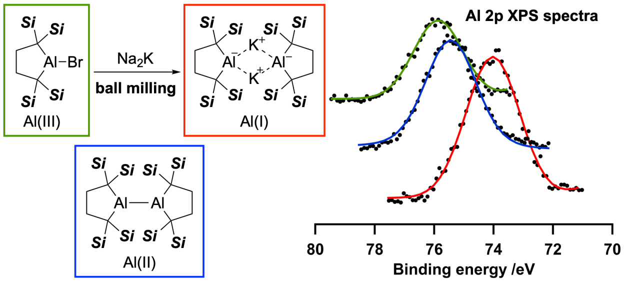

https://doi.org/10.26434/chemrxiv-2023-9h7z1 **ORCID:** https://orcid.org/0000-0002-3665-5311 Content not peer-reviewed by ChemRxiv. **License:** CC BY-NC-ND 4.0